Available online at www.sciencedirect.com

SCIENCE DIRECT®

Journal of Organometallic Chemistry 665 (2003) 107–113

Journal of Organometallic Chemistry

www.elsevier.com/locate/jorganchem

Regulation of electron donating ability to metal center: isolation and characterization of ruthenium carbonyl complexes with *N*,*N*- and/or *N*,*O*-donor polypyridyl ligands

Dai Ooyama [a,c,*], Takanori Kobayashi [a], Kazushi Shiren [b,c], Koji Tanaka [b,c,*]

[a] *Faculty of Education, Fukushima University, Kanayagawa, Fukushima 960-1296, Japan*
[b] *Institute for Molecular Science, Myodaiji, Okazaki 444-8585, Japan*
[c] *CREST, Japan Science and Technology Corporation (JST), Tokyo, Japan*

Received 18 July 2002; received in revised form 1 October 2002; accepted 29 October 2002

Abstract

Polypyridyl ruthenium(II) dicarbonyl complexes with an *N*,*O*- and/or *N*,*N*-donor ligand, $[Ru(pic)(CO)_2Cl_2]^-$ (**1**), $[Ru(bpy)(pic)(CO)_2]^+$ (**2**), $[Ru(pic)_2(CO)_2]$ (**3**), and $[Ru(bpy)_2(CO)_2]^{2+}$ (**4**) (pic = 2-pyridylcarboxylato, bpy = 2,2′-bipyridine) were prepared for comparison of the electron donor ability of these ligands to the ruthenium center. A carbonyl group of $[Ru(L1)(L2)(CO)_2]^n$ (L1, L2 = bpy, pic) successively reacted with one and two equivalents of OH^- to form $[Ru(L1)(L2)(CO)(C(O)OH)]^{n-1}$ and $[Ru(L1)(L2)(CO)(CO_2)]^{n-2}$. These three complexes exist as equilbrium mixtures in aqueous solutions and the equilibrium constants were determined potentiometrically. Electrochemical reduction of **2** in CO_2-saturated $CH_3CN–H_2O$ at −1.5 V selectively produced CO.

Keywords: Ruthenium; X-ray structures; Polypyridyl complexes; Carbonyl; Regulation of electron property; Electrochemistry

1. Introduction

There have been numerous reports of ruthenium(II) polypyridyl complexes [1], which show characteristic ligand-localized redox reactions [2]. Ruthenium carbonyl complexes with 2,2′-bipyridine (bpy) such as $[Ru(bpy)_2(CO)_2]^{2+}$ and $[Ru(bpy)(CO)_2Cl_2]$ have attracted much interest in the view points of the catalytic activity toward the reduction of CO_2 by utilizing the ligand-localized redox reactions as the electron sources [3]. We have prepared a series of $[Ru(bpy)_2(CO)X]^n$ (X = CO_2, C(O)OH, CO, CHO, CH_2OH, CH_3, $C(O)OCH_3$, and $C(O)CH_3$) as the possible reaction intermediates of multi-electron reduction of CO_2 [4,5]. Although the change of Ru–X bond character in $[Ru(bpy)_2(CO)X]^n$ has been discussed [4,5], substitution of bpy by other polypyridyl ligands is expected to give more serious influences on not only the redox potentials but also the reactivity of the complexes. In the present work with respect to a series of *cis*-$[Ru(L1)(L2)(CO)_2]^n$ (L1, L2 = 2-pyridylcarboxylato (pic), 2,2′-bipyridine), *cis*(CO),*trans*(Cl)-$[Ru(pic)(CO)_2Cl_2]^-$ (**1**) and *cis*-$[Ru(bpy)(pic)(CO)_2]^+$ (**2**) were newly prepared in addition to the known complexes (*cis*-$[Ru(pic)_2(CO)_2]$ (**3**) and *cis*-$[Ru(bpy)_2(CO)_2]^{2+}$ (**4**)) for comparison of the electron donor ability of the ligands to the Ru center.

2. Experimental

2.1. Materials

Ruthenium trichloride was purchased from Furuya Metals. Reagents 2,2′-bipyridine, 2-pyridylcarboxylic acid, tetraethylammonium chloride, tetra-*n*-butylammonium chloride (reagent grade), and tetra-*n*-butylammonium perchlorate (TBAP, electrochemical grade) of Nacalai Tesque, silver nitrate and potassium hexafluorophosphate (extra pure grade) of Wako Pure Chemicals

---

* Corresponding authors. Fax: +81-24-5483181
E-mail address: ooyama@educ.fukushima-u.ac.jp (D. Ooyama).

PII: S0022-328X(02)02072-7

were used without purification. Methanol and EtOH were HPLC grade and used without further purification. Acetonitrile for electrochemical measurements was distilled over CaH_2 under nitrogen just prior to use. Compounds $[Ru(CO)_2Cl_2]_n$, *cis*(CO),*trans*(Cl)-[Ru(bpy)$(CO)_2Cl_2$], and *cis*-[Ru(bpy)$_2(CO)_2](PF_6)_2$ (**4**) were prepared according to the literature methods [6,7].

2.2. Measurements

Elemental analysis of the products was performed at Chemical Material Center in Institute for Molecular Science. IR spectra were recorded on a Shimadzu FT-IR 8100 Fourier transform infrared spectrophotometer. ^{1}H- and ^{13}C-NMR spectra were measured with a JEOL EX-270 spectrometer. Cyclic voltammetry was carried out in CH_3CN under N_2 or in CH_3CN–H_2O (3%) under CO_2 with a three-electrode system and a CH Instruments, Inc., CHI 620A electrochemical analyzer interfaced to an IBM-compatible PC. The working and counter electrodes were Pt plates, and Ag–$AgNO_3$ (0.01 M) was used as a reference electrode. All potentials are reported in volts versus SCE containing 0.1 M TBAP as a supporting electrolyte. In all experiments, the potential scan rate was 0.1 V s^{-1} and the concentrations of the complexes were 1 mmol dm^{-3}. Reduction of carbon dioxide was carried out under controlled-potential electrolysis in a CO_2-saturated CH_3CN–H_2O (9:1 v/v) solution by using a CHI 620A electrochemical analyzer. Carbon monoxide evolved in the gaseous phase was analyzed by a Shimadzu GC-8A gas chromatograph equipped with a thermal conductivity detector and employed a 2 m column filled with Molecular Sieve 13X at 40 °C using He as the carrier gas. The amount of HCOOH produced in the reduction was measured by a Shimadzu IP-3A isotachophoretic analyzer. The potentiometric measurements were performed with a DKK-TOA HM-60S pH meter fitted with a DKK-TOA GST-5311C glass pH combination electrode at 25 °C. The experimental solutions, adjusted to 0.100 M in ionic strength by addition of KNO_3, were titrated with 0.100 M standard KOH. Equilibrium constants among three species ($[Ru(L1)(L2)(CO)_2]^n$, $[Ru(L1)(L2)(CO)(C(O)OH)]^{n-1}$, and $[Ru(L1)(L2)(CO)(CO_2)]^{n-2}$) were determined potentiometrically in aqueous solutions containing 4.0×10^{-4} M of $[Ru(L1)(L2)(CO)_2]^n$.

2.3. Synthesis of complex

2.3.1. $(R_4N)[Ru(pic)(CO)_2Cl_2]$ (R = Et: **1**, ^{n}Bu: **1′**)

A methanolic solution (5 cm^3) of Hpic (0.50 g) was degassed by bubbling N_2 for 30 min, and $[Ru(CO)_2Cl_2]_n$ (0.50 g) was added to the solution. The mixture was refluxed with stirring under N_2 atmosphere for 45 min. The reaction vessel was cooled to room temperature (r.t.) and then was allowed to stand at 3 °C overnight. The reaction mixture was evaporated to dryness under reduced pressures, and the residue was dissolved in water (5 cm^3). Addition of a saturated aqueous solution of Et_4NCl to the aqueous solution resulted in a pale yellow precipitate, which was collected by filtration and washed with cold water, and then dried under vacuum. Tetra-*n*-butylammonium (^{n}Bu$_4$N) salt was obtained by the addition of ^{n}Bu$_4$NCl instead of Et_4NCl. $(Et_4N)[Ru(pic)(CO)_2Cl_2]$ (**1**); yield, 0.45 g (43%). IR (KBr disk): ν(C≡O) at 2047 and 1973 cm^{-1}, $\nu_{as}(CO_2)$ at 1667 cm^{-1}, $\nu_s(CO_2)$ at 1339 cm^{-1}. NMR (^{1}H, Me_2SO-d_6): δ 8.86 (H_6), 8.17 (H_4), 8.02 (H_3), 7.77 (H_5), (^{13}C, Me_2SO-d_6): δ 198.20, 197.77 (*C*≡O), 170.30 (*C*=O), 151.27 (overlapping), 139.70, 128.00, 125.91 (pyridyl carbon). Anal. Found: C, 39.80; H, 4.95; N, 5.74. Calc. for $C_{16}H_{24}Cl_2N_2O_4Ru$: C, 40.01; H, 5.04; N, 5.83%. (^{n}Bu$_4$N)$[Ru(pic)(CO)_2Cl_2]$ (**1′**); Yield: 0.55 g (42%). IR (KBr disk): ν(C≡O) at 2053 and 1983 cm^{-1}, $\nu_{as}(CO_2)$ at 1646 cm^{-1}, $\nu_s(CO_2)$ at 1350 cm^{-1}.

2.3.2. $[Ru(bpy)(pic)(CO)_2]PF_6 \cdot 0.25H_2O$ (**2**·0.25H_2O)

$[Ru(bpy)(CO)_2Cl_2]$ (0.10 g) and Hpic (0.10 g) were dissolved in H_2O (80 cm^3). After the mixture was stirred at r.t. for 15 min, $AgNO_3$ (0.03 g, two equivalents) was added to the solution, and then the mixture was refluxed for 8 h. Gray precipitate of AgCl was removed by filtration through a Celite column, and the yellow–orange filtrate was concentrated to ca. 10 cm^3 under reduced pressures. Addition of a saturated aq. solution of KPF_6 (2 cm^3) to the solution resulted in an ivory precipitate. The precipitate was collected by filtration, and then washed with cold water and ether. Recrystallization was achieved from hot EtOH–C_3H_6O; Yield: 0.07 g (50%). IR (KBr disk): ν(C≡O) at 2089 and 2027 cm^{-1}, $\nu_{as}(CO_2)$ at 1680 cm^{-1}, $\nu_s(CO_2)$ at 1337 cm^{-1}. NMR (^{1}H, Me_2SO-d_6): δ 6.56–8.25 (12H), (^{13}C, Me_2SO-d_6): δ 192.44, 191.73 (*C*≡O), 170.62 (*C*=O), 157.54, 155.22, 154.50, 148.45, 148.25, 147.55, 141.85, 141.12, 129.78, 128.88, 128.34, 127.41, 125.41, 124.71 (pyridyl carbon). Anal. Found: C, 36.85; H, 2.19; N, 7.16. Calc. for $C_{18}H_{12}F_6N_3O_4PRu \cdot 0.25H_2O$: C, 36.97; H, 2.15; N, 7.18%.

2.3.3. *cis*-$[Ru(pic)_2(CO)_2]$ (**3**)

Although the compound has been prepared [8], we adopt an alternative method to prepare the complex. After an aq. solution (10 cm^3) of Hpic (0.50 g) was degassed by bubbling N_2 for 30 min, $[Ru(CO)_2Cl_2]_n$ (0.20 g) was added to the solution. The mixture was heated at reflux for 2 h. Then, the reaction vessel was cooled to 3 °C and allowed to stand at the temperature overnight. Pale yellow crystals deposited were collected by filtration and washed with cold water and then dried under vacuum; Yield: 0.16 g (44%). Elemental analysis, IR and NMR (^{1}H, ^{13}C) spectral data agreed well with those in a previous report [8].

2.4. X-ray structure determination

2.4.1. $(Et_4N)[Ru(pic)(CO)_2Cl_2]$ (1)

The single crystals of **1** were obtained directly from the reaction mixture. A yellow prismatic crystal of **1** having approximate dimensions of 0.50 × 0.25 × 0.25 mm was mounted on a glass fiber with epoxy resin. All data were collected on a Rigaku AFC5S diffractometer with graphite monochromated Mo–K_α radiation ($\lambda = 0.71069$ Å). The data were collected using the $\omega-2\theta$ scan technique to a maximum 2θ value of 55.0°. Empirical absorption correction based on azimuthal scans of several reflections was applied. The data were corrected for Lp effects. The structure was solved by heavy-atom Patterson methods [9] and refined on F by full-matrix least-squares technique; all calculations were performed using the TEXSAN [10] crystallographic software package. Carbon atoms of the tetraethylammonium cation were disordered in two positions with equal population parameters. Therefore, non-hydrogen atoms of the cation were not included in the refinements. The rest hydrogen atoms were fixed at the calculated positions. Because of the disorder, hydrogen atoms of the cation were omitted. Crystallographic parameters are summarized in Table 1 and selected bond lengths and angles are listed in Table 2.

Table 1
Crystallographic data for $(Et_4N)[Ru(pic)(CO)_2Cl_2]$ (**1**) and $[Ru(bpy)(pic)(CO)_2]PF_6$ (**2**)

	1	**2**·$0.25H_2O$
Chemical formula	$C_{16}H_{24}Cl_2N_2O_4Ru$	$C_{18}H_{12.5}F_6N_3O_{4.25}PRu$
Formula weight	480.35	584.85
Temperature (K)	289	173
Crystal system	Triclinic	Triclinic
Space group	$P\bar{1}$	$P\bar{1}$
Unit cell parameters		
a (Å)	9.819(2)	11.7738(5)
b (Å)	13.988(3)	16.2882(7)
c (Å)	7.724(2)	22.0275(9)
α (°)	99.98(3)	82.499(4)
β (°)	97.13(3)	87.373(6)
γ (°)	95.92(2)	89.805(5)
V (Å^3)	1028.3(5)	4183.7(3)
Z	2	8
Reflections measured	4710	18 111
Observations	3833 ($I > 3\sigma(I)$)	18110 (all)
Parameters	197	1198
R	0.044 [a]	0.059 [c]
R_w	0.072 [b]	0.126 [d]

[a] $R = \Sigma\,||F_o| - |F_c||/\Sigma\,|F_o|$.
[b] $R_w = \{\Sigma_w(|F_o| - |F_c|)^2/\Sigma_w F_o^2\}^{1/2}$.
[c] $R = \Sigma(F_o^2 - F_c^2)/\Sigma F_o^2$.
[d] $R_w = \{\Sigma_w(F_o^2 - F_c^2)^2/\Sigma_w(F_o^2)^2\}^{1/2}$.

Table 2
Selected bond lengths (Å) and angles (°) for **1** and **2**·$0.25H_2O$

Bond lengths		Bond angles	
1			
Ru1–Cl1	2.383(1)	Cl1–Ru1–Cl2	174.15(4)
Ru1–Cl2	2.395(1)	O3–Ru1–N1	78.5(1)
Ru1–O3	2.082(3)	C1–Ru1–C2	89.3(2)
Ru1–N1	2.107(3)	Ru1–C1–O1	177.7(5)
Ru1–C1	1.873(5)	Ru1–C2–O2	177.6(5)
Ru1–C2	1.834(5)		
C1–O1	1.145(6)		
C2–O2	1.146(6)		
2·$0.25H_2O$			
Ru1–O3	2.076(2)	O3–Ru1–N1	78.68(9)
Ru1–N1	2.118(2)	N2–Ru1–N3	78.34(9)
Ru1–N2	2.109(2)	C1–Ru1–C2	88.0(1)
Ru1–N3	2.074(2)	Ru1–C1–O1	174.6(3)
Ru1–C1	1.906(3)	Ru1–C2–O2	177.6(3)
Ru1–C2	1.901(3)		
C1–O1	1.124(4)		
C2–O2	1.135(4)		

2.4.2. $[Ru(bpy)(pic)(CO)_2]PF_6$ (2)

The single crystals of **2**·$0.25H_2O$ were also obtained directly from the reaction mixture. A yellow prismatic crystal of **2**·$0.25H_2O$ having approximate dimensions of 0.50 × 0.50 × 0.20 mm was mounted on a glass fiber. All data were collected on a Rigaku/MSC Mercury CCD diffractometer with graphite monochromated Mo–K_α radiation ($\lambda = 0.71070$ Å). The data were collected to a maximum 2θ value of 55.0°. A total of 720 oscillation images were collected. A first sweep of data was done using ω scans from −70.0 to 110.0° in 0.50° step, at $\chi = 45.0°$ and $\phi = 0.0°$. A second sweep of data was performed using ω scans from −70.0 to 110.0° in 0.50° step, at $\chi = 45.0°$ and $\phi = 90.0°$. The exposure rate was 10.0 s deg^{-1}, and the detector swing angle was 19.6°. The data were corrected for Lp effects. Systematic absences in the collected diffraction data were consistent with space group $P\bar{1}$ (No. 2). The structure was solved by direct methods [11] and refined on F^2 by full-matrix least-squares technique. All non-hydrogen atoms were refined anisotropically. Hydrogen atoms bound to carbon were fixed at the calculated positions. Non-coordinated water's hydrogen atoms were not modeled in the structure. Crystallographic parameters are summarized in Table 1 and selected bond lengths and angles are listed in Table 2.

3. Results and discussion

3.1. Synthesis and structure

Two synthetic routes are available for polypyridyl ruthenium(II) carbonyl complexes: one is introduction of CO followed by polypyridyl into metal centers, the other is incorporation of CO into polypyridyl ruthenium(II) complexs. Haukka and his coworkers extensively prepared mono-bipyridine derivatives of ruthenium(II) carbonyl complexes through $[Ru(CO)_3Cl_2]_2$ [12–14]. Keene and Meyer reported numerous ruthenium carbonyl complexes with bipyridine derivatives via polypyridyl ruthenium complexes [6,15–17]. Recently, $[Ru(pic)_2(CO)_2]$ was obtained by the one-pot reaction of $Ru_3(CO)_{12}$ with Hpic in toluene by Sasaki and Xu [8]. In the present work, we successfully isolated Et_4N^+ (**1**) and $^nBu_4N^+$ (**1′**) salts of a mono-pic complex as precursors of **2** and **3**, and **1** was used for an X-ray diffraction study (Fig. 1). Two geometrical isomers (A and B in Chart 1) of *cis*(CO)-$[Ru(bpy)(CO)_2Cl_2]$ were isolated and those crystal structures have been revealed [14]. Although another isomer C (Chart 1) is expected to exist in addition to A and B in case of *cis*(CO)-$[Ru(pic)(CO)_2Cl_2]^-$, only A form was confirmed, and neither type B nor C was detected in **1** and **1′** in the solid state and in solutions. Two Ru–C–O bond angles of $[Ru(pic)(CO)_2Cl_2]^-$ are nearly linear (Table 2), and the C–O and Ru–Cl bond lengths are similar to those of $[Ru(bpy)(CO)_2Cl_2]$ and $[Ru(bppi)(CO)_2Cl_2]$ (bppi = 3,6-bis(2-pyridyl)pyridazine) [14,18]. On the other hand, unsymmetrical chelate of pic gives substantial different effects on the two Ru–CO bonds of **1**; the Ru–C(2) bond length of 1.834 Å *trans* to the O atom is shorter than the Ru–C(1) bond length of 1.873 Å *trans* to the N atom. The Ru–O(3) bond length (2.082 Å) is shorter than the Ru–N(1) (2.107 Å) in good accordance with the above relationship between the Ru–C(1) and the Ru–C(2).

Attempts of introduction of bpy to **1** gave only dark blue unidentified deposits. The complex **2**, therefore, was prepared by the reaction of Hpic with $[Ru(bpy)(CO)_2Cl_2]$ (Scheme 1), and only the type D of the two possible isomers D and E was obtained (Chart 2 and Fig. 2). The unit cell contains four crystallographically independent molecules of **2** and one water molecule. Two complex cations of the four independent molecules form hydrogen bondings with the solvating water molecule. The terminal (O(4)) and the coordinated (O(11)) oxygen atoms in the carboxylato groups of the two complex cations lie close to the water oxygen atom (O(17)) with distances of 2.756 (O(4)···O(17)) and 2.812 Å (O(11)···O(17)), respectively. Bond lengths and angles of the four independent cations showed no significant differences. As shown in Table 2, the metrical parameters in the metal carbonyl moieties are similar to those in $[Ru(pic)_2(CO)_2]$ (**3**) and $[Ru(bpy)_2(CO)_2]^{2+}$ (**4**) [8,19]. The O–Ru–N angle in the pic five-membered ring (78.68°) and the N–Ru–N one in the bpy five-membered ring (78.34°) are also close to those in $[Ru(pic)_2(CO)_2]$ (**3**) and $[Ru(bpy)_2(CO)_2]^{2+}$ (**4**) [8,19].

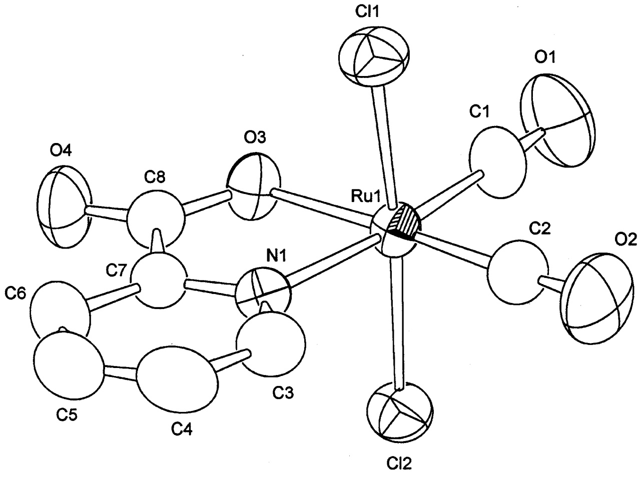

Fig. 1. Crystal structure of $[Ru(pic)(CO)_2Cl_2]^-$ (**1**) with atom labeling. Hydrogen atoms are omitted for clarity.

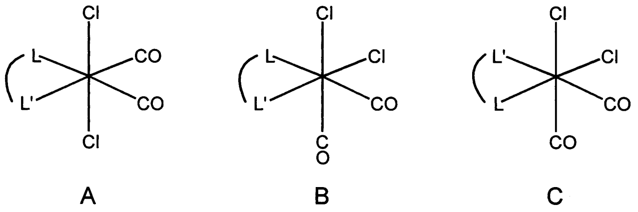

Chart 1.

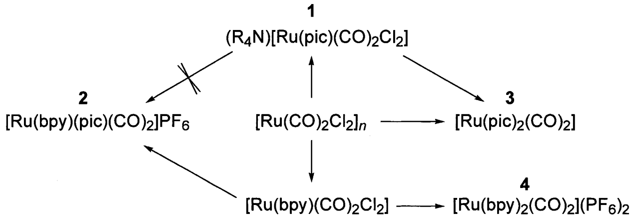

Scheme 1.

3.2. Comparison of electron donating ability of the ligands

It is well known that $[Ru(bpy)_2(CO)_2]^{2+}$ (**4**) exists as equilibrium mixtures with $[Ru(bpy)_2(CO)(C(O)OH)]^+$ and $[Ru(bpy)_2(CO)(CO_2)]^0$ in aqueous solutions (Eq. (1)). The amphoteric character of $[Ru(bpy)_2(CO)(C(O)OH)]^+$ plays the key role in the reversible conver-

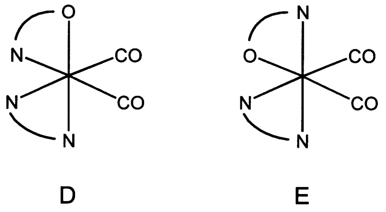

Chart 2.

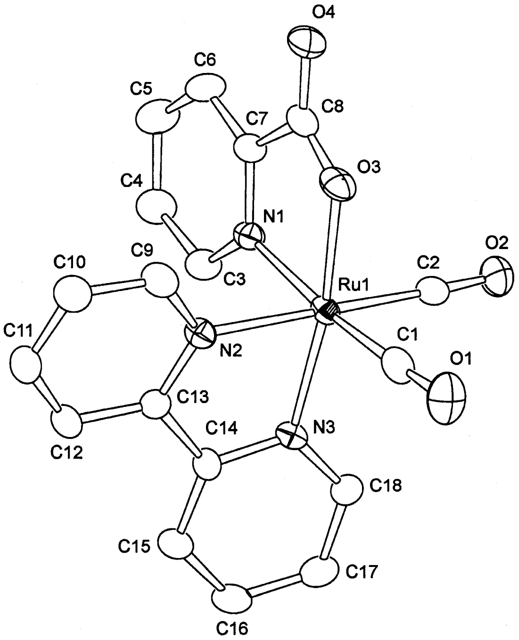

Fig. 2. Crystal structure of $[Ru(bpy)(pic)(CO)_2]^+$ (**2**) with atom labeling. Hydrogen atoms are omitted for clarity.

sion between CO and CO_2 on the metal [20].

$$[Ru(bpy)_2(CO_2)]^{2+} \underset{H^+}{\overset{OH^-}{\rightleftharpoons}} [Ru(bpy)_2(CO)(C(O)OH)]^+$$

$$\underset{H^+}{\overset{OH^-}{\rightleftharpoons}} [Ru(bpy)_2(CO)(CO_2)]^0 \qquad (1)$$

In accordance with Eq. (1), electronic absorption spectra and potentiometric pH titration of **2** and **3** also showed two successive acid–base equilibria in water at room temperature (Eqs. (2) and (3)) [21]. The equilibrium constants of Eqs. (2) and (3) were determined by potentiometric pH titration [22], and the results are summarized in Table 3.

$$[Ru(L1)(L2)(CO)_2]^n + OH^-$$

$$\overset{K_1}{\rightleftharpoons} [Ru(L1)(L2)(CO)(C(O)OH)]^{(n-1)} \qquad (2)$$

$$[Ru(L1)(L2)(CO)(C(O)OH)]^{(n-1)} + OH^-$$

$$\overset{K_2}{\rightleftharpoons} [Ru(L1)(L2)(CO)(CO_2)]^{(n-2)} + H_2O \qquad (3)$$

Distribution curves of $[Ru(bpy)(pic)(CO)X]^n$ ($X = CO$, $n = +1$; $X = C(O)OH$, $n = 0$; $X = CO_2$, $n = -1$) and $[Ru(pic)_2(CO)X]^n$ ($X = CO$, $n = 0$; $X = C(O)OH$, $n = -1$; $X = CO_2$, $n = -2$), together with $[Ru(bpy)_2(CO)X]^n$ ($X = CO$, $n = +2$; $X = C(O)OH$, $n = +1$; $X = CO_2$, $n = 0$) [23] calculated from the equilibrium constants K_1 and K_2, are shown in Fig. 3. For $[Ru(bpy)_2(CO)X]^n$, X = CO species predominates in a pH range less than 7.5, and the carboxylato form reaches the maximum distribution of 78% at pH 8.8. On the other hand, the carbonyl species of **2** and **3** remain as the main form up to pH 9 and 10, respectively. The corresponding carboxylato species of **2** and **3** become the maximum distribution at pH 9.5 and pH 10.5, respectively. The decrease of the K_1 and K_2 values in the order of $[Ru(bpy)_2(CO)X]^n > [Ru(bpy)(pic)(CO)X]^n > [Ru(pic)_2(CO)X]^n$ is reasonably ascribed to the strong electron donating ability of mono-anionic pic compared with neutral bpy. Indeed, the ν(CO) bands of these complexes showed the same tendency: **4** (2093, 2039 cm^{-1}) > **2** (2089, 2027 cm^{-1}) > **3** (2064, 2000 cm^{-1}). Concentration of the aqueous solution of **2** at pH 9.5 precipitated a mixture of $[Ru(bpy)(pic)(CO)_2]^+$ and $[Ru(bpy)(pic)(CO)(C(O)OH)]^0$ [24] with about a 1:4 ratio based on the comparison of the intensity of ν(CO) bands of the IR spectra, whereas pure $[Ru(bpy)_2(CO)(C(O)OH)]^+$ was isolated as a triflate salt under similar procedures. Moreover, concentration of aqueous solution of **3** at pH 10 selectively precipitated the original carbonyl complex probably due to less solubility of neural **3** compared with mono-anionic $[Ru(pic)_2(CO)(C(O)OH)]^-$ in an aqueous solution. Although we could not obtain the IR spectra of $[Ru(pic)_2(CO)(C(O)OH)]^-$, the comparison of the ν(CO) bands between [Ru(bpy)(pic)(CO)(C(O)OH)] (1937 cm^{-1}) and $[Ru(bpy)_2(CO)(C(O)OH)]^+$ (1960 cm^{-1}) [25] also indicated the strong electron donor ability of the bpy-pic combination compared with the bpy-bpy one.

Table 3
Equilibrium constants for $[Ru(L1)(L2)(CO)_2]^n$ [a]

Complex	K_1 (mol^{-1} dm^3)	K_2 (mol^{-1} dm^3)
$[Ru(bpy)_2(CO)_2]^{2+}$ (**4**)	1.32×10^5 [b]	2.27×10^4 [b]
$[Ru(bpy)(pic)(CO)_2]^+$ (**2**)	9.76×10^3	1.39×10^4
$[Ru(pic)_2(CO)_2]$ (**3**)	9.88×10^2	1.25×10^3

[a] $T = 25$ °C and $I = 0.100$ (KNO_3).

[b] Ref. [23].

3.3. Redox behavior

Cyclic voltammogram (CV) of **1** showed a reversible oxidation wave corresponding to the $Ru^{III/II}$ couple at 1.48 V, whereas no reduction wave emerged in the range of the potential window. On the other hand, the CV of **2** shows successive one-electron reduction at −1.15 and −1.44 V (Fig. 4a). Introduction of CO_2 into the solution by bubbling increased the peak currents of the cathodic waves. Moreover, an addition of water to the solution under CO_2 caused catalytic currents at potentials more negative than −1.1 V (Fig. 4c), suggesting that the reduced form of **2** has an ability to reduce CO_2 in the presence of protons. In fact, the electrolysis of **2** at −1.5 V in $CH_3CN–H_2O$ (9:1 v/v) under CO_2 produced CO as the two-electron reduction product of CO_2. However, black solids gradually deposited out of the electrolyte solution, and the cathodic currents of the reduction of CO_2 almost ceased after an electricity of 16 C was

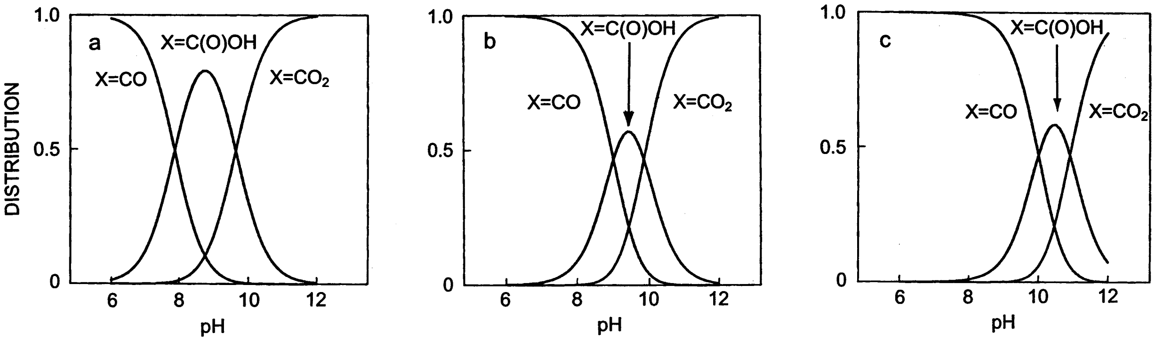

Fig. 3. Distribution curves of $[Ru(L1)(L2)(CO)X]^n$ (X = CO, C(O)OH, and CO_2) in H_2O at various pHs at 25 °C: (a) $[Ru(bpy)_2(CO)X]^n$; (b) $[Ru(bpy)(pic)(CO)X]^n$; (c) $[Ru(pic)_2(CO)X]^n$.

consumed. Thus, **2** showed an ability to catalyze reduction of CO_2 but the complex was not stable enough to endure the present electrolysis conditions.

The CV of **3** displays irreversible reduction at −1.68 V in CH_3CN under N_2 (Fig. 4b). It is worthy of note that the pattern of the CV of **3** is quite resemble to that of **4**, which undergoes irreversible reduction at −1.0 V [26]. Thus, the replacement of two bpy of $[Ru(bpy)_2(CO)_2]^{2+}$ (**4**) with two pic resulted in negative (cathodic) shift of the redox potentials of the complex by 700 mV. However, the peak currents of the irreversible cathodic wave at −1.68 V of **3** hardly increased upon addition of H_2O under CO_2 atmosphere, indicating low activity toward the reduction of CO_2 (Fig. 4d). Thus, the catalytic activity of the reduction of CO_2 decreases in the order $[Ru(bpy)_2(CO)_2]^{2+}$ (**4**) > $[Ru(bpy)(pic)(CO)_2]^{+}$ (**2**) > $[Ru(pic)_2(CO)_2]^{0}$ (**3**), though the order mentioned in Section 3.2 must be reverse with respect to the conversion from CO_2 to CO on Ru under less protic conditions. It is worthy of note that CO production in the catalytic cycle of the reduction of CO_2 catalyzed by $[Ru(bpy)_2(CO)_2]^{2+}$ (**4**) is caused by the reductive Ru–CO bond cleavage with maintaining the $Ru(bpy)_2(CO)$ framework under the electrolysis conditions [27]. On the other hand, gradual decomposition of the catalyst in the reduction of CO_2 catalyzed by $[Ru(bpy)(pic)(CO)_2]^{+}$ (**2**) probably results from occurrence of both Ru–CO bond cleavages and dechelation or dissociation of the pic ligand, because $[Ru(pic)_2(CO)_2]$ (**3**) essentially does not have the catalytic ability toward the reduction of CO_2. Thus, the view that chelation of the Ru-pic framework is not stable enough to make selective Ru–CO bond cleavage under electrolysis conditions reasonably explains the order of the catalytic activity of **2**, **3**, and **4** toward the reduction of CO_2.

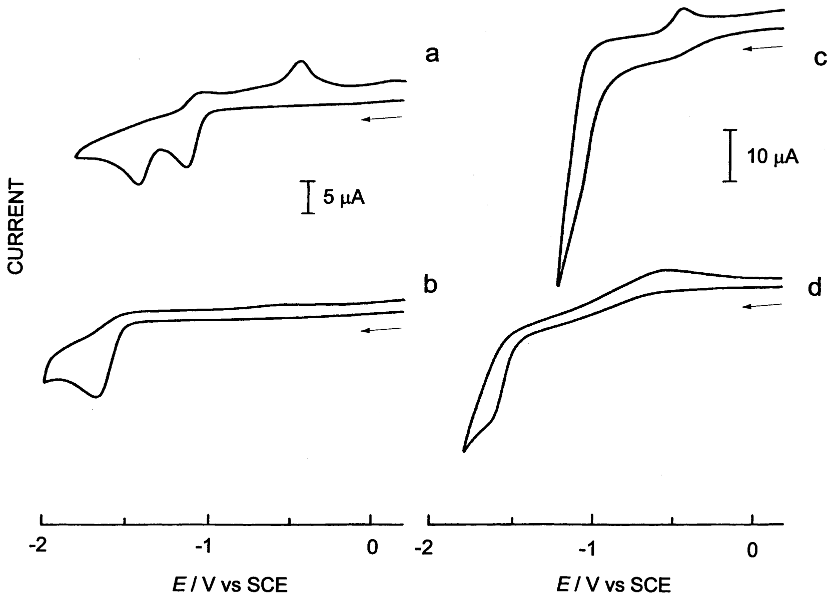

Fig. 4. Cyclic voltammograms of **2** and **3** at 25 °C: (a) **2** in CH_3CN–N_2; (b) **3** in CH_3CN–N_2; (c) **2** in CH_3CN–H_2O/CO_2; (d) **3** in CH_3CN–H_2O/CO_2.

4. Supplementary material

Crystallographic data for the structural analyses have been deposited with the Cambridge Crystallographic Data Centre, CCDC Nos. 178720–21 for compounds **1** and **2**, respectively. Copies of this information may be obtained free of charge from The Director, CCDC, 12 Union Road, Cambridge CB2 1EZ, UK (Fax: +44-1223-336033; e-mail: deposit@ccdc.cam.ac.uk or www: http://www.ccdc.cam.ac.uk).

References

[1] (a) L.-N. Ji, X.-H. Zou, J.-G. Liu, Coord. Chem. Rev. 216–217 (2001) 513;
(b) S. Fanni, T.E. Keyes, C.M. O'Connor, H. Hughes, R. Wang, J.G. Vos, Coord. Chem. Rev. 208 (2000) 77;
(c) C.G. Garcia, J.F. De Lima, N.Y.M. Iha, Coord. Chem. Rev. 196 (2000) 219;
(d) M.D. Ward, Int. J. Photoenergy 1 (1999) 121;
(e) L.-N. Ji, J.-G. Liu, B.-H. Ye, Mater. Sci. Eng. C10 (1999) 51;
(f) J.A. Treadway, B. Loeb, L.R. Lopez, P.A. Anderson, F.R. Keene, T.J. Meyer, Inorg. Chem. 35 (1996) 2242;
(g) F. Millett, B. Durham, Met. Ions Biol. Syst. 27 (1991) 223;
(h) T.J. Meyer, Pure Appl. Chem. 62 (1990) 1003;
(i) T.J. Meyer, J. Electrochem. Soc. 131 (1984) 221C.

[2] V. Balzani, A. Juris, M. Venturi, S. Campagna, S. Serroni, Chem. Rev. 96 (1996) 759.

[3] (a) S. Chardon-Noblat, A. Deronzier, R. Ziessel, Collect. Czech. Chem. Commun. 66 (2001) 207;
(b) S. Chardon-Noblat, G.H. Cripps, A. Deronzier, J.S. Field, S. Gouws, R.J. Raymond, F. Southway, Organometallics 20 (2001) 1668;
(c) E. Fujita, M. Chou, K. Tanaka, Appl. Organomet. Chem. 14 (2000) 844;
(d) S. Chardon-Noblat, P. Da Costa, A. Deronzier, M. Haukka, T.A. Pakkanen, R. Ziessel, J. Electroanal. Chem. 490 (2000) 62;
(e) T. Mizukawa, K. Tsuge, H. Nakajima, K. Tanaka, Angew. Chem. Int. Ed. Engl. 38 (1999) 362;
(f) R. Ziessel, Stud. Surf. Sci. Catal. 114 (1998) 219;
(g) S. Chardon-Noblat, A. Deronzier, R. Ziessel, D. Zsoldos, J. Electroanal. Chem. 444 (1998) 253;
(h) R. Ziessel, L. Toupet, S. Chardon-Noblat, A. Deronzier, D. Matt, J. Chem. Soc. Dalton Trans. (1997) 3777;
(i) S. Chardon-Noblat, A. Deronzier, R. Ziessel, D. Zsoldos, Inorg. Chem. 38 (1997) 5384;
(j) D.H. Gibson, B.A. Sleadd, M.S. Mashuta, J.F. Richardson, Organometallics 16 (1997) 4421;
(k) H. Nakajima, Y. Kushi, H. Nagao, K. Tanaka, Organometallics 14 (1995) 5093;
(l) S. Chardon-Noblat, M.-N. Collomb-Dunand-Sauthier, A. Deronzier, R. Ziessel, D. Zsoldos, Inorg. Chem. 33 (1994) 4410;
(m) M.-N. Collomb-Dunand-Sauthier, A. Deronzier, R. Ziessel, Inorg. Chem. 33 (1994) 2961;
(n) M.-N. Collomb-Dunand-Sauthier, A. Deronzier, R. Ziessel, J. Chem. Soc. Chem. Commun. (1994) 189;
(o) M.R.M. Bruce, E. Megehee, B.P. Sullivan, H.H. Thorp, T.R. O'Toole, A. Downard, J.R. Pugh, T.J. Meyer, Inorg. Chem. 31 (1992) 4864;
(p) H. Tanaka, H. Nagao, S.-M. Peng, K. Tanaka, Organometallics 11 (1992) 1450;
(q) J.R. Pugh, M.R.M. Bruce, B.P. Sullivan, T.J. Meyer, Inorg. Chem. 30 (1991) 86;
(r) K. Tanaka, H. Miyamoto, T. Tanaka, Chem. Lett. (1988) 2033;
(s) H. Ishida, H. Tanaka, K. Tanaka, T. Tanaka, Chem. Lett. (1987) 597;
(t) H. Ishida, K. Tanaka, T. Tanaka, Chem. Lett. (1985) 405.

[4] K. Toyohara, K. Tsuge, K. Tanaka, Organometallics 14 (1995) 5099.

[5] D. Ooyama, T. Tomon, K. Tsuge, K. Tanaka, J. Organomet. Chem. 619 (2001) 299.

[6] P.A. Anderson, G.B. Deacon, K.H. Haarmann, F.R. Keene, T.J. Meyer, D.A. Reitsma, B.W. Skelton, G.F. Strouse, N.C. Thomas, J.A. Treadway, A.H. White, Inorg. Chem. 34 (1995) 6145.

[7] J.M. Kelly, C.M. O'connell, J.G. Vos, Inorg. Chim. Acta 64 (1982) L75.

[8] L. Xu, Y. Sasaki, J. Organomet. Chem. 585 (1999) 246.

[9] P.T. Beurskens, G. Admiraal, G. Beurskens, W.P. Bosman, S. Garcia-Granda, R.O. Gould, J.M.M. Smits, C. Smykalla, PATTY: the DIRDIF program system, Technical Report of the Crystallography Laboratory, University of Nijmengen, The Netherlands, 1992.

[10] TEXSAN: Crystal Structure Analysis Package, Molecular Structure Corporation, 1985, 1992, and 1999.

[11] SIR-92: A. Altomare, M.C. Burla, M. Camalli, M. Cascarano, C. Giacovazzo, A. Guagliardi, G. Polidori, J. Appl. Crystallogr. 27 (1994) 435.

[12] E. Eskelinen, M. Haukka, T. Venäläinen, T.A. Pakkanen, M. Wasberg, S. Chardon-Noblat, A. Deronzier, Organometallics 19 (2000) 163.

[13] M. Haukka, P. Hirva, S. Luukkanen, M. Kallinen, M. Ahlgrén, T.A. Pakkanen, Inorg. Chem. 38 (1999) 3182.

[14] M. Haukka, J. Kiviaho, M. Ahlgrén, T.A. Pakkanen, Organometallics 14 (1995) 825.

[15] J.A. Treadway, T.J. Meyer, Inorg. Chem. 38 (1999) 2267.

[16] N.C. Fletcher, F.R. Keene, J. Chem. Soc. Dalton Trans. (1998) 2293.

[17] G.F. Strouse, P.A. Anderson, J.R. Schoonover, T.J. Meyer, F.R. Keene, Inorg. Chem. 31 (1992) 3004.

[18] G. De Munno, G. Denti, G. De Rosa, G. Bruno, Acta Crystallogr. Sect. C 44 (1988) 1193.

[19] H. Tanaka, B.-C. Tzeng, H. Nagao, S.-M. Peng, K. Tanaka, Inorg. Chem. 32 (1993) 1508.

[20] (a) K. Tanaka, K. Tsuge, Trend Inorg. Chem. 4 (1996) 145;
(b) K. Tanaka, Adv. Inorg. Chem. 43 (1995) 409.

[21] Complexes **2** and **3** in H_2O behave as dibasic acids on titration with aqueous KOH solutions in a similar manner as $[Ru(bpy)_2(CO)_2]^{2+}$ (**4**). Thus, these data would support the existence of two successive equilibria in aqueous alkaline solutions of both **2** and **3**.

[22] A.E. Martell, R.J. Motekaitis, Determination and Use of Stability Constants, 2nd ed., VCH, New York, 1992.

[23] K. Tanaka, M. Morimoto, T. Tanaka, Chem. Lett. (1983) 901.

[24] In the IR spectrum, the ν(CO) and ν(C(O)OH) bands of [Ru(bpy)(pic)(CO)(C(O)OH)] were observed at 1937 and 1642 cm^{-1}, respectively.

[25] H. Ishida, K. Tanaka, M. Morimoto, T. Tanaka, Organometallics 5 (1986) 724.

[26] H. Nagao, T. Mizukawa, K. Tanaka, Inorg. Chem. 33 (1994) 3415.

[27] K. Tanaka, Bull. Chem. Soc. Jpn. 71 (1998) 17.